PHYSICAL REVIEW C VOLUME 9, NUMBER 4 APRIL 1974

Neutron-proton scattering at a few MeV

E. Lomon*
Laboratory for Nuclear Science, Massachusetts Institute of Technology, Cambridge, Massachusetts 02139

and

Richard Wilson†
Department of Physics, Harvard University, Cambridge, Massachusetts 02138

(Received 20 August 1973; revised manuscript received 28 January 1974)

In this paper we reanalyze the *np* scattering data at a few MeV; we confirm, as previously suggested by Hopkins and Breit, that the *np* interaction models all predict the angular distribution well. Any further angular-distribution measurements must be very precise to contribute further to our knowledge.

[NUCLEAR REACTIONS *np* scattering $E \approx 10$ MeV; calculated $\sigma(\theta)$, $P(\theta)$, σ_T, correlated experiments.]

I. INTRODUCTION

There are many reasons for reanalyzing our knowledge of the *np* cross section at a few MeV. Among them is the use of the cross section as a standard. One use of this cross section standard is a measurement of fast neutron flux—particularly for reactors using fast neutrons such as the liquid metal fast breeder. In such an application, neutron fluxes are obtained by measuring the proton recoils from a hydrogenous radiator. This number is proportional both to the flux and to the *np* differential cross section at a c.m. angle of 180°. Secondly we may be interested in the theory of the *np* interaction and thirdly, we may wish to use the deuteron as a neutron target in elementary particle physics experiments, and hence need to know the *np* scattering parameters. All these reasons are coupled. If, for example, we wish to know the cross section at an energy at which it has not been measured, we can interpolate using theory if we are convinced that the cross section does not have an unknown oscillation or resonance.

II. DATA

In the region of incident neutron energies E_{lab} from 100 keV to 10 MeV there are several measurements of the total cross section for *np* scattering with an accuracy of 1% or better. Since the compilation of MacGregor, Arndt, and Wright[1] there have been other data.[2-4] Total cross sections are fairly easy to measure and are therefore more reliable and more accurate than differential cross sections. There are only a few differential cross-section measurements below 14 MeV and none of enough reliability and accuracy to be of any significance. Therefore, anyone who wants to know the 180° differential cross section below 14 MeV must use theory or a combination of theory and experiment.

In addition to the total cross-section data, there exist data below 60 MeV on *np* angular distributions,[1,5] on polarization,[1,6] on correlation coefficients,[1] and on triple scattering.[1]

III. INTERPOLATION USING BASIC THEORY

Hopkins and Breit[7] use the theoretical knowledge of the momentum dependence of the *np* interaction at threshold. If the *np* potential has a short range, the various phase shifts are expected to behave as $k^{(2L+1)}$ where k is the wave number and L the angular momentum in units of $\hbar$. The scattering of nucleons by nucleons has been extensively studied at incident (laboratory) energies from zero up to 400 MeV. At the lower part of this range, the phase shifts are small, and Breit and Hopkins argue that they can be determined at low energies by the threshold behavior.

We find it convenient to parametrize the angular distribution in *np* scattering by either one of two parameters:

$$R = \sigma_{180}/\sigma_{90} \tag{1}$$

$$R' = 4\pi\sigma_{180}/\sigma_T . \tag{2}$$

At low energies where S phases and S, P interference dominate, $R = R'$. At higher energies, where D phases become important, $R' < R$.

Neutron beams at an energy close to 14.1 MeV can be conveniently produced by the reaction $^2H + ^3H \rightarrow n + ^4He$ and there have been many measurements at this energy.[8-14] The values of R derived therefrom are listed in Table I together with the values of R given by various models.[7,15-19] In Ref. 20 the full angular distributions are plotted.

If we examine the earlier measurements (Refs. 8–13) we find an average value

$$R = 1.079 \pm 0.011, \quad \chi^2 = 2.1, \tag{3}$$

five degrees of freedom. If we include the discordant value $R = 1.031 \pm 0.01$ found in Ref. 14 we find

$$R = 1.051 \pm 0.007, \quad \chi^2 = 13.8, \tag{4}$$

six degrees of freedom.

Opinions differ on how to handle a discordant set of data; one could throw out the data of Ref. 14 since it is 4 standard deviations from the earlier data or one could use the combined average and increase the error estimate by a factor of 3 to allow for the difference in internal and external consistency. Then one obtains

$$R = 1.051 \pm 0.021 \text{ at } 14.1 \text{ MeV}. \tag{5}$$

If S and P phase shifts have threshold behavior and higher waves are negligible (the fact that R is close to one tends to suggest that P phases are small and thus may have threshold behavior), then

$$R = 1 + AE. \tag{6}$$

The direct interpolation procedure then consists of fitting A at 14.1 MeV by the experimentally determined value. We find from Eqs. (5) and (6) that below 5 MeV, R is known to better than 0.7%.

But this interpolation is sufficiently important that the validity of extrapolating the threshold behavior to energies of 14 MeV must be independently confirmed. Doubts already arise when considering the S phases above 5 MeV; both the singlet and triplet np scattering lengths are large, so that the effective range term [Eq. (11)] is relatively large. The variation with energy of the total cross section indicates this, and phase-shift analyses confirm it.[1,15] Further doubts arise from considering the $^3P_0$ phase shift which deviates considerably from threshold behavior above 25 MeV. Therefore, the data at 14.1 MeV and higher energies do not, by themselves, determine the coefficients of the threshold dependence or the phases below 14 MeV.

An extreme form of this possible ambiguity is given by the older interpolation of Gammel.[16] Assuming the absence of P waves and fitting to the 90-MeV data, he obtained

$$R = 1 + 2(E/90)^2. \tag{7}$$

This interpolation predicts the low-energy results indicated in Table I and Fig. 1.

However, the *deviation* from threshold behavior is dominated by the long-range part of the interaction. The one-pion-exchange part of the potential (OPEP) dominates for the long-range part of the np interaction since the π meson has the smallest mass of any strongly interacting particle. We know the pion-nucleon coupling constants and hence OPEP. This is confirmed by analysis of high-energy low momentum transfer data.[1] At low energies, the P phases are determined primarily by the OPEP. The S phases also depend upon details of the core in the np interaction, but this dependence is constrained by a combination of the total cross-section data and the high-energy data.

IV. USE OF A MODEL FOR INTERPOLATION

In order to do better than the simple interpolation[7] and to take account of all the points noted above, we use models that build in the OPEP behavior as well as the threshold limit and which fit all the data well (in general $\chi^2/\chi_0^2 \approx 1$–2 for all data up to 350 MeV). We have matched the low-energy data even better by adjusting the parameters in each of three separate types of models; the Hamada-Johnson (HJ) potential,[17] the Bressel-Kerman (BKR) soft-core potential,[18] and the boundary-condition models of Feshbach and Lomon[19] (BCM) (various fits for several values of the percentage of D-state and pion-nucleon coupling constant). The Yale potential[15] used by Hopkins and Breit[7] is similar to the Hamada-Johnston potential.[17] All these models have the theoretical one-pion-exchange (OPEP) form at large interaction distances.

The choice of a variety of models provides an indication of the degree to which errors in the high-energy data can propagate down. To test the propagation of the errors in the low-energy data, we have varied the BCM parameters to match the extremes of the experimental errors on the various experimentally measured np parameters.

In Table I we show these various model predictions for R. The difference between the "unconstrained" energy-dependent phase-shift analysis of Ref. 1 and the "constrained" analysis is that in the latter case the analysis was constrained to give a positive value for the S, D "coupling" parameter so that it could match the low-energy data on this parameter given by the binding energy of the deuteron. With the unrealistic "unconstrained" phase-shift analysis omitted, the models

TABLE I. Angular dependence near 14.1 MeV.

Source and reference	$\sigma(180°)/\sigma(90°)$	χ^2 of model fit to data [a]
Experiment, Ref. 8	1.10 ±0.03	
Experiment, Ref. 9	1.093 ± 0.022	
Experiment, Ref. 10	1.08 ±0.016	
Experiment, Ref. 11	1.06 ±0.023	
Experiment, Ref. 12	1.04 ±0.06	
Experiment, Ref. 13	1.06 ±0.06	
Experiment, Ref. 14	1.031 ± 0.010	
Phase-shift analysis, Ref. 1 "unconstrained" phases	1.014	
Phase-shift analysis, Ref. 1 "constrained" phases	1.055	
Phase-shift analysis, Refs. 7, 15	1.055	
Threshold extrapolation without P waves, Ref. 16	1.05	
Hard-core potential, Ref. 17 [b]	1.066	154
Flat-core potential, Ref. 18 fitted to a_t [c]	1.066	$391 + \chi^2(\epsilon)$ [d]
Flat-core potential, Ref. 18 fitted to ϵ [c]	1.066	356
Boundary-condition model, Ref. 19, case 5, [e] 5.20% D state, $(g_\pi)^2 = 14.94 \times (4\pi)$	1.080	218
Boundary-condition model, Ref. 19, case 15, [e] 7.55% D state, $(g_\pi)^2 = 14.95 \times (4\pi)$	1.082	303
Boundary-condition model, Ref. 19, case 5 [f] with $(4\pi)^{-1} g_\pi^2 = 14.4$ (4.94% D state)	1.077	228
Boundary-condition model, Ref. 19, case 5 [g] with poor low-energy fit	1.080	225

[a] The model comparison is with ϵ, a_t, and Q of Table II and with 94 data points at energies below 59.35 MeV taken from Refs. 1–6. Data with poor absolute normalization were omitted.

[b] To increase the precision of Ref. 17 in fitting a_s, a_t, and ϵ we have used M_N(reduced) = 938.903 MeV, $M_\pi(T=1) = 137.54$ MeV, and $M_\pi(T=0) = 139.74$ MeV. The hard-core radius is $0.343\hbar/M_\pi C$.

[c] The model of Ref. 17 is unable to fit a_t and ϵ simultaneously (implying a wrong value of the effective range). To precisely fit a_t we have used a core height $V_c(T=0, S=1) = 463.5$ MeV. To precisely fit ϵ we have used $V_c(T=0, S=1) = 466.91$ MeV. In both cases we use $V_c(T=1, S=0) = 699.96$ MeV for a precise fit of a_s.

[d] Due to the ultra-high experimental precision of ϵ, the contribution to χ^2 from this source in this model choice is huge and essentially irrelevant. The predicted value is $\epsilon = 2.2505$.

[e] To increase the precision of a_s we have used $f_{001} = 1.875\,64$ instead of the published value of 1.875 60.

[f] To compensate for the change in g_π we use $f_{001} = 1.859\,165$ and $f_{01} = 1.705\,92$ instead of the published values.

[g] To *decrease* the precision of a_s ($\Delta\chi^2 = 7$) we use $f_{001} = 1.875\,45$.

all give at 14.1 MeV

$$1.05 < R < 1.082 . \tag{8}$$

The last two entries show the effects of decreasing the pion-nucleon coupling constant g_π to a low value or of spoiling the $^1S_0$ scattering-length fit by changing the boundary condition. We see the effects are smaller than model differences.

To be thorough one would perform a complete error analysis to determine the extent to which the errors on the low- and high-energy data propagate, through the parameters in the models, to changes in R and R' at low energy. This is a formidable task. However, as shown in Table I, we find that small adjustments to the models to match extremes of the low-energy cross-section data make smaller changes in the predictions than the differences between the models. Also, the models used provide a variety of fits to the high-energy data, thus indicating the range of error propagation downward.

The energy dependence of R according to the models is shown in Fig. 1, with the experimental values of R superposed. We note that the simple linear interpolation is not correct, but use of it will not lead to a large error.

As shown by Fig. 2, the models predict the linear behavior of Eq. (6) below 5 MeV, but already at 14 MeV they show a deviation from the simple behavior confirming the need for the more complex analysis. The assumption of Ref. 16 is inconsistent with the finite P wave predicted at

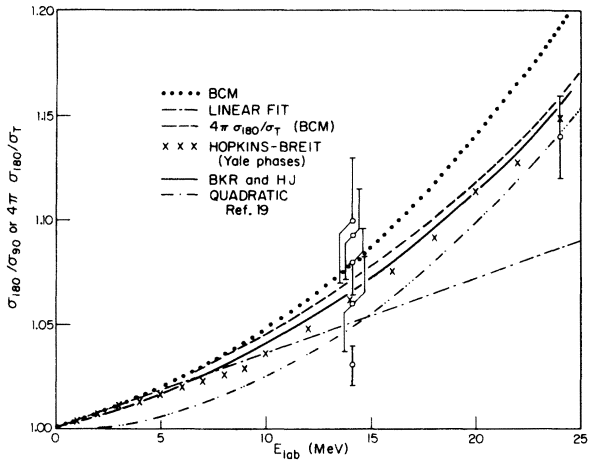

FIG. 1. *np* angular distribution coefficients. The experimental values of R [Eq. (1)] at 14.1 MeV are those of Refs. 9, 10, 11, and 14 and are tabulated in Table I. At 24 MeV the experimental value of R is extrapolated from the experiment of L. N. Rothenberg, Phys. Rev. C 1, 1226 (1970). The curves are predictions of models or extrapolation formulas as indicated by the legend. The points marked with an × are obtained from Yale phase shifts via Ref. 17. The dashed curve is R [Eq. (2)] as predicted by the BCM potential. The HJ, BKR, and BCM potentials are the versions indicated by Table I footnotes b; c, a_t fit; and e for 5.20% D state, respectively.

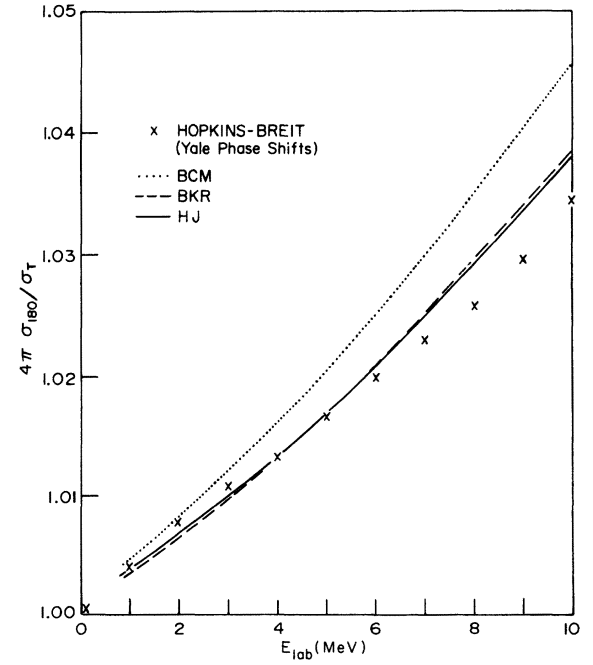

FIG. 2. R' [Eq. (2)] predictions for *np* scattering at low energy. The model curves and points are as in Fig. 1.

low energies by the models and their prediction for R is inconsistent with Eq. (7) below 5 MeV.

In spite of the considerable differences between the models for the short-range part of the interaction, they predict a narrow band of values for R.

The most extreme in this respect is the prediction of the boundary-condition model. We believe the reason is that this model at low energies fails to fit the $^3P_0$ phase shift well (see Fig. 11 of Ref. 19) and it is the interference of this amplitude with the S amplitude that gives rise to the angular distribution. We also note that the Hopkins and Breit recipe gives a different energy dependence of R and R' than the other models. At $E_{lab} > 3.2$ MeV they use phase-shift analyses which are required to provide phase shifts varying smoothly with energy. The difference of this curve from one generated by a theoretically reasonable model gives one indication of the variation possible in the energy-dependent analysis of the experiments and this partially substitutes for a complete error analysis.

In general, we believe that the Hamada-Johnston model, adjusted as we have to fit the low-energy data, gives the best recipe.

V. POLARIZATION

The polarization at low energies has been shown by Clementel and Villi[21] to be proportional to

$$P \propto 2\sin\delta(^3P_0)\sin[\delta(^3P_0) - (^3S_1)] + 3\sin\delta(^3P_1)\sin[\delta(^3P_1) - \delta(^3S_1)]$$

and since $\delta(^3S_1)$ is large and the P-state phases are small, this is approximately

$$P \propto -\sin\delta(^3S_1)[2\delta(^3P_0) + 3\delta(^3P_1)] \,. \tag{10}$$

All the phase-shift analyses show that

$$\delta(^3P_1) \simeq -\tfrac{1}{2}\delta(^3P_0)$$

and hence, a large degree of cancellation occurs in the polarization. Small errors in $\delta(^3P_0)$ lead to larger fractional errors in the polarization. Although the $\cos\theta$ term in the differential cross section[22] has some cancellation from the $^3P_0$ and $^3P_1$ contributions, there is also a large contribution from $^1P_1$ and $^1S_0$ interference. Hence, the fractional error in the ratio σ_{180}/σ_{90} is only proportional to the fractional error in the P phase shifts without an enhancement due to cancellations. Moreover, because of the growing importance of OPEP, these model errors decrease as the energy is reduced.

The polarization is, therefore, sensitive to details of the models. The results are displayed in Fig. 3. It is evident that the polarization prediction of the Hamada-Johnston potential is good;

the prediction of the BCM model is inferior and we attribute this to the poor fit to the $^3P_0$ phase shift already noted above. Fortunately this phase has less importance in the differential cross section.

We also note in Fig. 3 the lack of smoothness of the predictions from Hopkins and Breit, due to the fact that they tie themselves to phase-shift analyses and not to a model.

VI. TOTAL CROSS SECTION AND BEST VALUES

The total cross section is measured at several energies from 500 keV to 30 MeV and is displayed in Fig. 4; in Fig. 5 we display $\sigma_T \times E$, which is easier to read in the region of 5 MeV where it is nearly constant.

At zero energy we know the cross sections from measurements; these are separated into singlet and triplet parameters by using coherent scattering and the use of the binding energy of the deuteron. These very low-energy parameters are listed in Table II. In the first column we show the "1970 best values" listed by Wilson.[20] Since then, the measurement of the coherent *np* scattering length by the measurement of the critical angle for reflection of neutrons by hydrocarbon mirrors has been revised by Koester and Nistler[23] leading to "1973 best values" shown in the second column of Table II. We have confidence in Koester's revised value, because he has also revised the measurement of the coherent scattering by carbon and, hence, the carbon total cross section. This now agrees with Houk's[24] careful work, enhancing our faith in Houk's total hydrogen cross section. However, we must ignore the discordant measurement of coherent *np* scattering by scattering on parahydrogen, which in any case has internal inconsistencies; but we note that including it and increasing the error to span the data has no effect on the major conclusion of this paper.

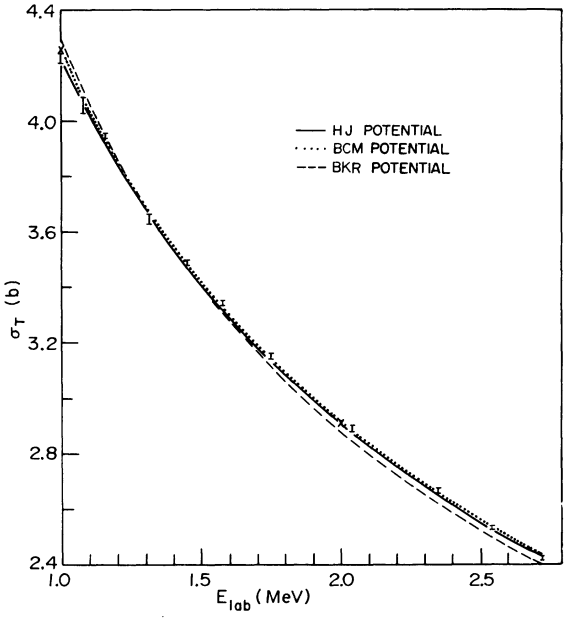

FIG. 4. *np* total cross section. The experimental data are tabulated in Ref. 1. The model curves and points are as in Fig. 1.

At low energies these can be used to calculate the cross section according to the *shape-independent* effective-range approximation

$$\sigma = \frac{3\pi}{k^2 + (\frac{1}{2}k^2 r_t - 1/a_t)^2} + \frac{\pi}{k^2 + [\frac{1}{2}k^2 r_s - 1/a_s]^2} \,. \quad (11)$$

$k^2 = (M\epsilon/\hbar^2)$ where M is the nucleon mass and we neglect the contributions of order k^4 in the ex-

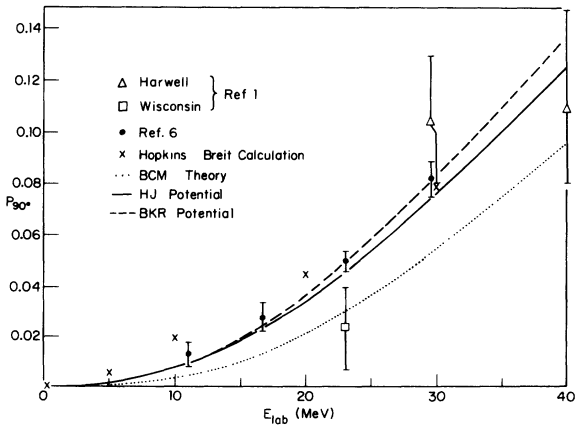

FIG. 3. *np* polarization. The data are from Refs. 1 and 6. The model curves and points are as in Fig. 1.

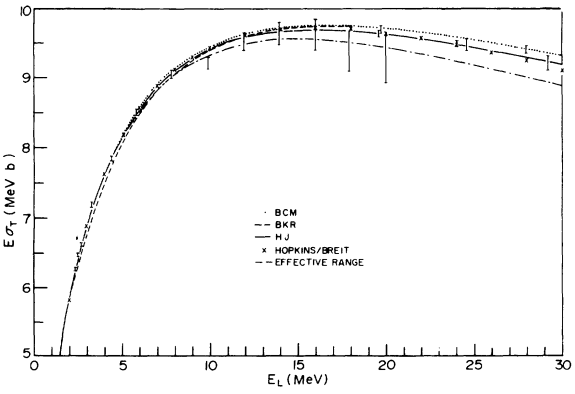

FIG. 5. *np* cross sections multiplied by the energy. The model curves are as in Fig. 1. The dash-dot curve is the effective-range prediction.

pansion of the S phase shift:

$$k\cot\delta_t = \frac{1}{a_t} + \tfrac{1}{2}k^2 r_t - P_t k^4 r_t^3 + \cdots \quad . \tag{12}$$

Higher partial waves are also neglected. In Table II the values of a_t, a_s, and r_t are determined from low-energy measurements and the deuteron binding energy ϵ; r_s is determined by fitting to experimental data at energies up to 2 MeV. In this detailed fitting, *theoretical* values of the omitted terms in the cross section are used for columns 1 and 2. In column 3, we list the "shape-independent parameters" (except for ρ_s). The calculation from the shape-independent formula is simple and forms a convenient reference. In Fig. 5 we see that this formula underpredicts σ_t by $\frac{1}{2}\%$ near 10 MeV. In Fig. 6 we plot the difference of the total cross section from the effective range formula for each model and for the data. This gives a convenient expanded scale.

VII. OTHER INFORMATION

Two other pieces of information confirm the general theoretical picture. There have been searches for fluctuations in the np total cross section as a function of energy. Early experimental claims have been convincingly refuted.[25]

Secondly, the photodisintegration of the deuterion by γ rays with energies from 2.5 to 6 MeV proceeds mainly by the electric dipole transition ($^3S \rightarrow {}^3P$). Using the approximation that the np force is short ranged, the cross section can be shown to depend primarily on the normalization of the ground-state deuteron wave function, and hence on the np triplet effective range. The triplet effective range $\rho_t(-\epsilon, -\epsilon)$ is found to be $(1.82 \pm 0.05)\times 10^{-13}$ cm and this is equivalent to $r_t = (1.83 \pm 0.05)\times 10^{-13}$ cm after a small correction is applied for the shape parameter. The equality of this with the number derived from np scattering confirms the short-range character of the potential as assumed in OPEP.

VIII. CONCLUSIONS AND RECIPE

We have seen that the theoretical models all give a good description of the low-energy data, and the np and pp intermediate-energy data, while satisfying theoretical requirements such as one-pion-exchange dominance at long range. Therefore, we can have confidence in the predictions. There are more theoretical constraints than used by Hopkins and Breit. The variety of models and data fits gives an estimate of the possible error propagation.

For those who wish to determine σ_{180}, to measure neutron intensity by means of proton recoils, we present two alternative simple recipes. Read σ_t from Figs. 4 or 5, or if more accuracy is desired, calculate σ_t from the simple effective-range formula and use Fig. 6. The Hamada-Johnston prediction is to be preferred and the accuracy should be $\pm\frac{1}{4}\%$. Then read R' from Fig. 2 to derive σ_{180}. Again, the Hamada-Johnston prediction is to be preferred, but we suggest assigning an error equal to the difference from the BCM model, leading to an over-all error in σ_{180} of less than $\frac{1}{2}\%$ up to 5 MeV; this error is a standard deviation. Alternatively experimental data can be used for σ_T combined with theory for R' as above.

At intermediate angles $\sigma(\theta)$ can be calculated accurately enough up to 10 MeV by assuming that it varies as $1 + a\cos\theta$ (i.e., neglecting D phases).

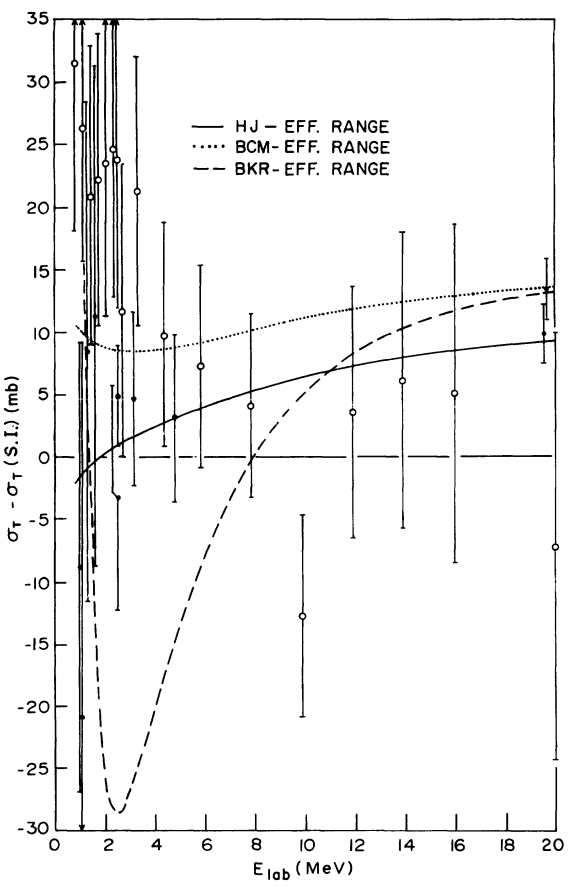

FIG. 6. The difference between model predictions of σ_T and the shape-independent effective-range value σ_T(S. I.). The models are as indicated in Fig. 1. The poor effective range of the BKR potential causes large deviation from σ_T(S. I.) below 8 MeV. The difference of experimental value of σ_T from σ_T(S. I.) is also plotted. The open circles represent the data of Ref. 3, in which the normalization is not adequate to predict the scattering lengths. The other data (filled circles) shows the trend to the shape-independent approximation.

TABLE II. Low-energy *np* parameters. The changes 1970–1973 are a revision of f due to changes in earlier results, and a change in r_{0s} with newer cross-section measurements and a revised energy scale for earlier measurements.

Parameters	1970 values	1973 values	Shape-independent fit
Binding energy of the deuteron ϵ (keV)	2224.644 ± 0.046	2224.644 ± 0.046	2224.644
Low-energy cross section σ_H (b)	20.436 ± 0.023	20.436 ± 0.023	20.436
Coherent scattering length $f = (3a_t + a_s)/2$ (fm)	−3.719 ± 0.004	−3.739 ± 0.003	−3.739
Triplet scattering length (derived) a_t (fm)	5.423 ± 0.005	5.414 ± 0.005	5.414
Singlet scattering length (derived) a_s (fm)	−23.712 ± 0.013	−23.719 ± 0.013	−23.719
Triplet effective range (derived) r_{0t} [$=\rho(0,-\epsilon)$] (fm)	1.761 ± 0.005	1.750 ± 0.005	1.7481
Singlet effective range (derived) r_{0s} (fm)	2.74 ± 0.05	2.76 ± 0.05	2.76
Ground-state effective range $\rho(-\epsilon,-\epsilon)$ (fm)	1.82 ± 0.05	1.82 ± 0.05	
Triplet effective range derived from $\rho(-\epsilon,-\epsilon)$ using model (fm)	1.83 ± 0.05	1.83 ± 0.05	
Quadrupole moment of the deuteron Q (fm)^2		0.278 ± 0.008 [a]	

[a] The ascribed uncertainty is due to the variations of electronic wave functions used in the analysis of the experiments.

A nuclear data committee[26] has recommended a remeasurement of the *np* angular distribution at these energies. We believe the accuracy of the measurements must be greater than the accuracy of this recipe for the measurements to be useful. At least it should be as accurate as this recipe purports to be, as an independent check of our analysis.

*Supported in part by the Atomic Energy Commission Contract No. AT(11-1)-3069.

†Supported in part by the National Science Foundation Contract No. GP38119.

[1]M. H. MacGregor, R. A. Arndt, and R. M. Wright, Phys. Rev. 182, 1714 (1969).

[2]J. C. Davis, K. A. Weaver, D. Hilscher, H. H. Barschall, and A. B. Smith, Phys. Rev. C 4, 1061 (1971).

[3]A. Langsford and P. J. Clements, in Neutron Standards and Flux Normalizations, Proceedings of the Symposium Held at Argonne National Laboratory, October, 1970 (unpublished), p. 5.

[4]J. C. Davis and H. H. Barschall, Phys. Lett. 27B, 636 (1968), (revised energy scale for some earlier data).

[5]T. G. Masterson, Phys. Rev. C 6, 690 (1972).

[6]G. S. Mutchler and J. E. Simmons, Los Alamos Report No. LA-DC-12432 (unpublished).

[7]J. C. Hopkins and G. Breit, Nucl. Data A9, 137 (1971).

[8]I. Busar, M. Cerineo, P. Tomas, and D. Miljanic, Fysika 1, 105 (1968).

[9]M. Tanaka, N. Koori, and S. Shirato, J. Phys. Soc. Jap. 28, 11 (1970). The absolute value of the cross section, not discussed in this paper, is revised in S. Shirato and K. Sartok, St. Paul's University, Tokyo, Japan Report No. RUP 73-7 (to be published).

[10]T. Nakamura, J. Phys. Soc. Jap. 15, 1359 (1960).

[11]J. D. Seagrave, Phys. Rev. 97, 757 (1955).

[12]J. C. Allred, A. H. Armstrong, and L. Rosen, Phys. Rev. 91, 90 (1953).

[13]H. H. Barschall and R. F. Taschek, Phys. Rev. 75, 1819 (1949).

[14]T. Arvieux and J. Pouve, Phys. Lett. 32B, 468 (1970).

[15]K. E. Lassila, M. H. Hull, Jr., H. M. Ruppel, F. A. MacDonald, and G. Breit, Phys. Rev. 126, 881 (1962).

[16]J. L. Gammel, in *Fast Neutron Physics*, edited by J. B. Marion and J. L. Fowler (Interscience, New York), Part II, p. 2185.

[17]T. Hamada and I. D. Johnston, Nucl. Phys. 34, 382 (1962).

[18]C. N. Bressel, A. K. Kerman, and B. Rouben, Nucl. Phys. A124, 624 (1969).

[19]E. L. Lomon and H. Feshbach, Ann. Phys. (N. Y.) 48, 94 (1968).

[20]R. Wilson, in Neutron Standards and Flux Normalizations, Proceedings of the Symposium Held at Argonne National Laboratory, October, 1970 (unpublished), p. 27.

[21]E. Clementel and C. Villi, Nuovo Cimento 5, 1166 (1957).

[22]H. Feshbach and E. Lomon, Phys. Rev. 102, 891 (1956), see Eqs. (50)–(52).

[23]L. Koester and W. Nistler, Phys. Rev. Lett. 27, 956 (1971).

[24]T. L. Houk, Phys. Rev. C 3, 1886 (1971).

[25]S. Cierjacks, in Neutron Standards and Flux Normalizations, Proceedings of the Symposium Held at Argonne National Laboratory, October 1970 (unpublished), p. 190.

[26]R. S. Caswell, Standards Subcommittee, National Bureau of Standards, private communication.